Designing the properties of dispersion-flattened photonic crystal fibers

Albert Ferrando, Enrique Silvestre, and Pedro Andrés

Departament d'Òptica, Universitat de València, E-46100 Burjassot, Spain

albert.ferrando@uv.es

Juan J. Miret

Departament d'Òptica, Universitat d'Alacant, E-03080 Alacant, Spain

Miguel V. Andrés

Institut de Ciència dels Materials, Universitat de València, E-46100 Burjassot, Spain

Abstract: We present a systematic study of group-velocity-dispersion properties in photonic crystal fibers (PCF's). This analysis includes a thorough description of the dependence of the fiber geometrical dispersion on the structural parameters of a PCF. The interplay between material dispersion and geometrical dispersion allows us to established a well-defined procedure to design specific predetermined dispersion profiles. We focus on flattened, or even ultraflattened, dispersion behaviors both in the telecommunication window (around 1.55 μm) and in the *Ti-Za* laser wavelength range (around 0.8 μm). We show the different possibilities of obtaining normal, anomalous, and zero dispersion curves in the above frequency domains and discuss the limits for the existence of the above dispersion profiles.

OCIS codes: (060.2270) Fiber characterization; (060.2280) Fiber design and fabrication; (060.2430) Fibers, single mode

References and links

1. A. Ferrando, E. Silvestre, J. J. Miret, P. Andrés, and M. V. Andrés, "Donor and acceptor guided modes in photonic crystal fibers," Opt. Lett. **25**, 1238-1330 (2000).
2. D. Mogilevtsev, T. A. Birks, and P. S. J. Russell, "Dispersion of photonic crystal fibers," Opt. Lett. **23**, 1662-1664 (1998).
3. M. J. Gander, R. McBride, J. D. C. Jones, D. Mogilevtsev, T. A. Birks, J. C. Knight, and P. S. J. Russell, "Experimental measurement of group velocity dispersion in photonic crystal fibers," Electron. Lett. **35**, 63-64 (1999).
4. P. J. Bennet, T. M. Monro, and D. J. Richardson, "Toward practical holey fiber technology: fabrication, splicing, modeling, and fabrication," Opt. Lett. **24**, 1203-1205 (1999).
5. A. Ferrando, E. Silvestre, J. J. Miret, J. A. Monsoriu, M. V. Andrés, and P. S. J. Russell, "Designing a photonic crystal fibre with flattened chromatic dispersion," Electron. Lett. **24**, 325-327 (1999).
6. J. Broeng, D. Mogilevtsev, S. E. Barkou, and A. Bjarklev, "Photonic crystal fibers: a new class of optical waveguides," Opt. Fib. Tech. **5**, 305-330 (1999).
7. A. Ferrando, E. Silvestre, J. J. Miret, and P. Andrés, "Nearly zero ultraflattened dispersion in photonic crystal fibers," Opt. Lett. **25**, 790-792 (2000).
8. E. Silvestre, M. V. Andrés, and P. Andrés, "Biorthonormal-basis method for the vector description of optical-fiber modes," J. Lightwave Technol. **16**, 923-928 (1998).

#37487 - $15.00 US Received November 05, 2001; Revised December 05, 2001

9. A. Ferrando, E. Silvestre, J. J. Miret, P. Andrés, and M. V. Andrés, "Full-vector analysis of a realistic photonic crystal fiber," Opt. Lett. **24**, 276-278 (1999).
10. A. Ferrando, E. Silvestre, J. J. Miret, P. Andrés, and M. V. Andrés, "Vector description of higher-order modes in photonic crystal fibers," J. Opt. Soc. Am. A **17**, 1333-1340 (2000).
11. D. Davidson, Optical-Fiber Transmission (E. E. Bert Basch, ed., Howard W. Sams & Co, 1987).

1 Introduction

One of the most appealing features of photonic crystal fibers (PCF's) is their high flexibility based on the particular geometry of their refractive index distribution. The transverse section of a PCF is a two-dimensional (2D) silica-air photonic crystal in which an irregularity of the refractive index, or defect, is generated. In PCF's guidance occurs in the region where the defect is located, which determines an effective PCF core. Analogously, one can define an effective PCF cladding constituted by the region surrounding the core, or defect area, that has the form of a perfectly periodic 2D photonic crystal. As compared to conventional fibers, it is apparent that PCF's enjoy a more complex geometrical structure because of their 2D photonic crystal cladding. This fact allows us to manipulate the geometrical parameters of the fiber (e.g., the air-hole radius a and the lattice period, or pitch, Λ of a 2D triangular photonic crystal cladding) to generate an enormous variety of different configurations.

The peculiarities of the guidance in the core depend on the nature of the defect, which can generate donor or acceptor guided modes by an analogous mechanism leading to impurity states in electronic crystals [1]. On the other hand, the functional form of the dispersion relation of guided modes is very sensitive to the 2D photonic crystal cladding. For this reason, one expects to be able to control, at least to some extent, the dispersion properties of guided modes by manipulating the geometry of the photonic crystal cladding. It was soon realized that PCF's exhibited dispersion properties very different than those corresponding to ordinary fibers. As an example, some PCF configurations presenting a point of zero dispersion well below the characteristic zero dispersion point of silica at $1.3\,\mu$m where found [2, 3, 4], as well as some other showing flattened dispersion profiles [5, 6, 7]. Since the number of different photonic crystal configurations is significant, one can deduce that it must be possible to elaborate a procedure to tailor the dispersion of PCF modes in an efficient way. The success in the achievement of such a procedure, that has to be necessarily smart and cannot be based on pure guesses, will ideally provide a useful design tool to determine the PCF geometrical parameters necessary to obtain a desired dispersion profile with specific characteristics. A first approach to design the dispersion properties of PCF's using a systematic procedure has been already suggested in Ref.[7].

The calculation of the dispersion properties of PCF modes requires a highly efficient numerical method. The dispersion coefficient D is proportional to the second derivative of the modal effective index with respect to the wavelength λ. For this reason, it is very sensitive to the precision with which the dependence of n_{eff} with λ is calculated. On the other hand, the calculation method has to provide a reasonable computational time for evaluating the dispersion curves of different configurations. Ideally, it should also be flexible to accommodate divers geometric proposals (such as different photonic-crystal lattice geometries, non-perfect lattices and holes, asymmetries, different materials, and so on) with a little effort. Here, we use a full-vector modal method developed by our own group to describe electromagnetic propagation in general systems with translational invariance [8], supplemented by the use of periodic boundary conditions for the transverse electromagnetic field [9]. Periodic boundary conditions, together with the fact that the propagation problem is formulated in a purely 2D framework, turn out to be crucial for the simplification of the method and the achievement of a versatile and efficient

#37487 - $15.00 US Received November 05, 2001; Revised December 05, 2001

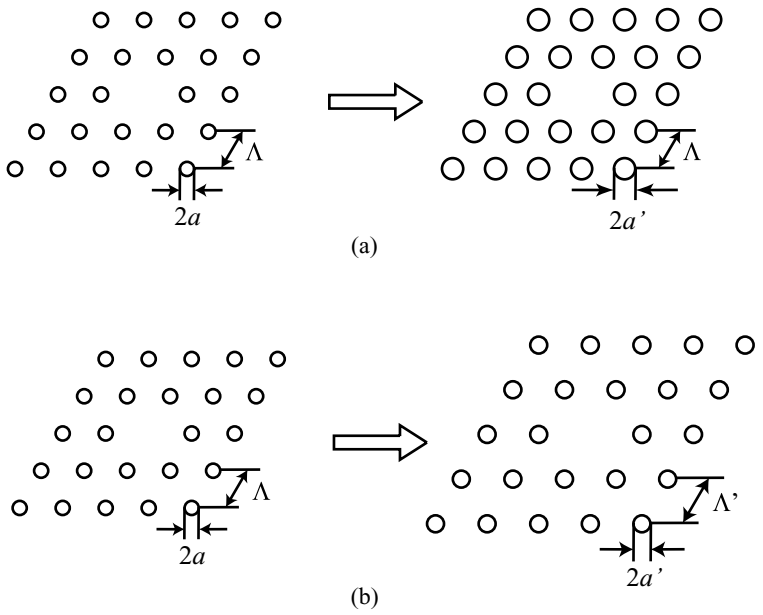

Fig. 1. Transformations of the lattice structure with the dimensionless parameters f and M: (a) two structures with different filling fraction f and same magnification M ($a/\Lambda \neq a'/\Lambda$); (b) two structures with different magnification M and same filling fraction f ($a/\Lambda = a'/\Lambda$).

algorithm [10]. At the same time, our approach permits to introduce the chromatic dispersion of the material in a natural way, without an extra cost in time or in precision. In this sense, this method provides a very reasonable balance between precision and computational time that makes it a perfect companion for the design procedure described in this paper, as we shall see.

2 Designing Procedure

In this paper, we will focus on the dispersion properties of triangular silica-air PCF's with circular holes, although our procedure can be easily adapted to other geometries and materials. Geometrically, a triangular lattice is characterized by the air-hole radius a and the lattice period, or pitch, Λ. However, in the design procedure we have recognized that it is more convenient to consider two alternate dimensionless parameters instead. First, we consider the so-called filling fraction f, defined as $f = (4\pi/3)(a/\Lambda)^2$, that involves the dimensionless ratio a/Λ and provides the proportion of air with respect to silica in the photonic crystal structure. A change in f produces a variation of the amount of air in the structure, as shown in Fig. 1(a). The second parameter we take into account is the magnification M, which simply consists in a simultaneous scale transformation of both a and Λ in the same amount, as shown in Fig. 1(b). In order to define M operatively, it is convenient to select a reference value of the pitch (in our case, we choose $\Lambda = 2.3\,\mu$m). The magnification M has also an appealing practical interest. In the pulling process during the fabrication of the fiber, M is the parameter that can be controlled in a natural way. This is so because, under optimal conditions, the pulling process should preserve the proportions of the original structure.

The definition of the dispersion coefficient of a PCF is

$$D \equiv -\frac{\lambda}{c}\frac{d^2 n_{\text{eff}}}{d\lambda^2}, \tag{1}$$

#37487 - $15.00 US
Received November 05, 2001; Revised December 05, 2001

where the effective refractive index of the mode is given by $n_{\rm eff} = \beta[\lambda, n_{\rm m}(\lambda)]/k_0$, β is the propagation constant, $k_0 = 2\pi/\lambda$ is the free-space wave number, and $n_{\rm m} = n_{\rm m}(\lambda)$ is the chromatic dispersion of the material, silica in this case. According to the above equation, there are two different sources of obtaining non-zero dispersion due to the existence of two different types of dependence of β on λ. One of them is originated by the explicit dependence of the propagation constant of the mode on λ and it occurs even if the material is, or it can be considered, non-dispersive ($n_{\rm m}(\lambda) = {\rm const}$). Since the dispersion generated in this way is not produced by the chromatic dispersion of the material but by the geometry of the PCF refractive index distribution that determines the dispersion relation of the guided mode, $\beta = \beta[\lambda, n_{\rm m}(\lambda) = {\rm const}]$, we call it geometrical dispersion. Its definition is, accordingly, the same as in Eq. (1) but supplemented with the condition that the material is non-dispersive; $D_{\rm g} \equiv D|_{n_{\rm m}(\lambda)={\rm const}}$. The second source of dispersion is certainly given by the implicit dependence of β on λ through the chromatic dispersion of the material, $n_{\rm m} = n_{\rm m}(\lambda)$. Consequently, this type of dispersion is called material dispersion, $D_{\rm m}$, and we calculate it as in Eq. (1) by substituting $n_{\rm eff}(\lambda)$ by $n_{\rm m}(\lambda)$.

Our design procedure is based on the possibility to approximate the real dispersion D by a sum of the geometrical and material dispersion [11];

$$D(\lambda) \approx D_{\rm g}(\lambda) + D_{\rm m}(\lambda). \tag{2}$$

The problem of designing the dispersion of a PCF becomes clearer when D is written in this way. The virtue of Eq. (2) is that permits to split both sources of dispersion into two different terms explicitly.

Since we consider air-silica PCF's, the chromatic dispersion of silica $n_{\rm m}(\lambda)$ is an input of the problem and consequently, so is $D_{\rm m}$. All the design power is stored in the geometrical dispersion, In this sense it is very important to recognize the following fact. The effective refractive index of a guided mode $n_{\rm eff}$, for the calculation of which we assume no material dispersion, *explicitly* depends on the photonic crystal cladding parameters, a and Λ, and the wavelength λ. Inasmuch as $n_{\rm eff}$ is a dimensionless function, this dependence can only occur through dimensionless ratios of these three parameters. For our discussion, it is convenient to take as independent parameters a/λ and Λ/λ, so that $n_{\rm eff} = n_{\rm eff}(a/\lambda, \Lambda/\lambda)$. This property determines the dependence of $D_{\rm g}$ on M completely. According to the definition of the geometrical dispersion, it is clear that under a scale transformation of λ, we obtain

$$D_{\rm g}(\lambda; M, f) = \frac{1}{M} D_{\rm g}(\frac{\lambda}{M}; f). \tag{3}$$

Consequently, it is enough to calculate the dispersion curve for one reference configuration (fixing the filling fraction f and setting $M = 1$, or equivalently, fixing a and $\Lambda = 2.3\,\mu m$) to analytically obtain all the family of dispersion curves parametrized by M, as shown in Fig. 2(a). The linear part of these curves modifies its slope and it is simulteanously shitfed when M is changed.

On the contrary, there is no simple analytical approach to predict the behavior of $D_{\rm g}$ with the filling fraction f. In practice, the only way to determine this dependence is by calculating $D_{\rm g}$ numerically. We thus start with a reference configuration, e.g. $M = 1$ (i.e., with $\Lambda = 2.3\,\mu$m) and evaluate the geometrical dispersion curves for different filling fractions f simply by changing a. The result is represented in Fig. 2(b). The remarkable feature of these curves is that, besides they are shifted, the slope of their linear part is approximately preserved when the filling fraction is changed. This property will show to be very helpful in the design process.

The design procedure is better visualized by means of a graphical representation of the geometrical, material and total dispersion. For convenience, the total dispersion is

#37487 - $15.00 US Received November 05, 2001; Revised December 05, 2001

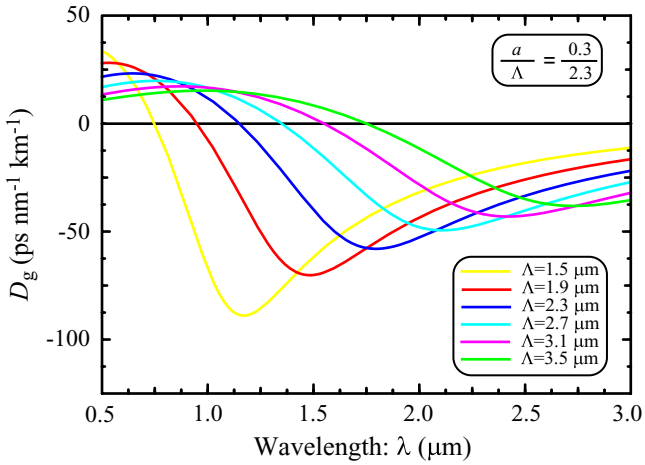

(a)

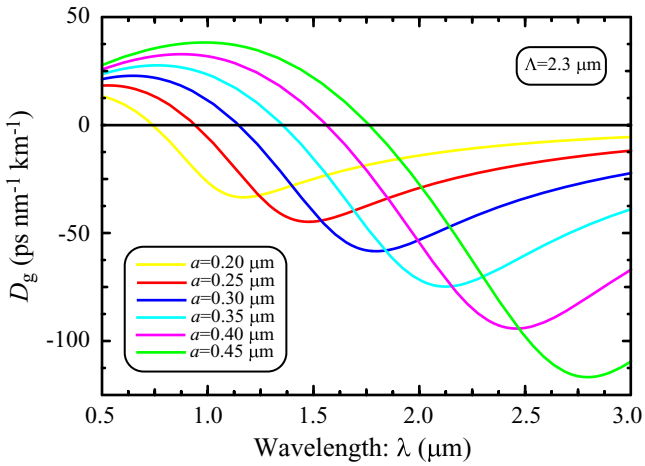

(b)

Fig. 2. Dependence of the geometrical dispersion curves on: (a) the magnification M; and (b) the filling fraction f.

#37487 - $15.00 US
Received November 05, 2001; Revised December 05, 2001

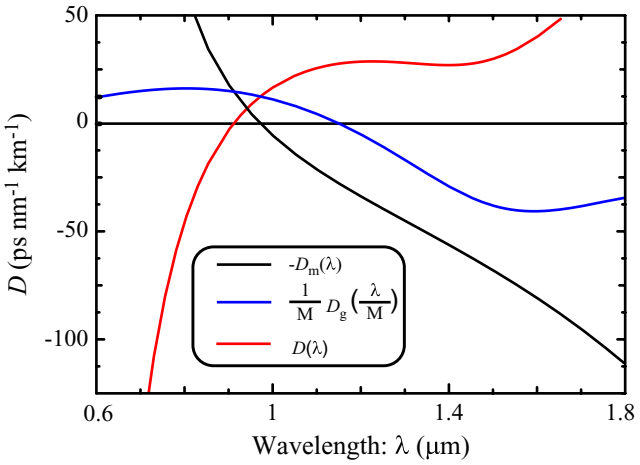

Fig. 3. The total dispersion D (red curve) is, in a first-order approximation, the result of substracting the sign-changed material dispersion $-D_{\rm m}$ (black curve) from the geometrical dispersion $D_{\rm g}$ (blue curve). A typical case exhibiting positive ultra-flattened dispersion in the 1.55 μm window is obtained.

calculated using Eq. (2), but written in a slightly different form,

$$D(\lambda) \approx D_{\rm g}(\lambda) - (-D_{\rm m}(\lambda)). \tag{4}$$

In Fig. 3, the curves corresponding to the geometrical dispersion $D_{\rm g}$, the sign-changed material dispersion $-D_{\rm m}$, and the total dispersion D, are represented in blue, black and red, respectively. According to Eq. (4), the red curve corresponding to total dispersion is obtained by subtracting the values of the black curve from the blue one.

With the previous ingredients, we can give a well-defined prescription to design PCF's with ultraflattened dispersion profiles. Ultraflattened dispersion possess a point with zero fourth-order dispersion located between the two consecutive extremes. Up to date, this behavior has been predicted to exist only in PCF's resulting in extremely wide nearly zero flattened dispersion profiles [7].

The key factor to achieve this particularly interesting dispersion property is the control of the slope of the linear part of $D_{\rm g}$. The sign-changed material dispersion $-D_{\rm m}$ is a smooth curve in most of the infrared region, so that it can be well approximated by a linear function around different λ's belonging to this region over pretty wide intervals. It is clear, in view of Fig. 3, that in the region of λ's in which the linear part of both the black and blue curves can be set parallel, the total dispersion will achieve an ideally perfect flattened behavior.

The strategy to obtain such a behavior is then straightforward. We start by determining the slope of the black curve at some specific wavelength. In the region where the material dispersion curve is smooth, this slope is approximately the same for a reasonably wide neighborhood around the specified wavelength. Once the slope of the $D_{\rm m}$ curve is fixed, we perform a scale transformation of $D_{\rm g}$ parametrized by the magnification M in such a way that provides an scaled $D_{\rm g}$ curve having a linear region with the same given slope. If the wavelength region (centered at the specified λ) where $D_{\rm m}$ behaves linearly overlaps the wavelength region of linear behavior of $D_{\rm g}$, we will obtain an ultraflattened total dispersion curve in the overlapping wavelength range.

This process fixes the value of M. However, it remains still one degree of freedom to play with, the filling fraction f. As shown in Fig. 2(b), note that a change in f does not alter the value of the slope of the linear part of $D_{\rm g}$. Therefore, if we proceed to change

#37487 - $15.00 US
Received November 05, 2001; Revised December 05, 2001

the value of f preserving the value of M obtained above, the difference between both curves will change, and also the overlapping range, but the parallelism condition will remain unaltered. This means that one simultaneously modifies the value of the total dispersion D and the width of the wavelength window where ultraflattened behavior occurs by acting on the filling fraction f. Since these two properties are not independent, one has the choice to select f either to obtain a desired value of D or to maximize the range of ultraflattened dispersion operation. In both cases, all possible configurations will provide ultraflattened dispersion profiles.

This ends the design procedure that gives the values of M and f providing a previously established ultraflattened dispersion behavior at a reference wavelength. The design procedure does not supply us with the exact parameters because it is based on an approximate expression for D (see Eq. (2)). If one is interested in a more accurate evaluation of M and f, one can undertake a second fine-tuning search of the actual parameters starting from their approximate values. This search is performed by calculating the real dispersion exactly, that is, by including the chromatic dispersion of the material explicitly in the determination of the dispersion relation of the mode (see Eq. (1)). Since the starting values are pretty close to the real ones, the fine-tuning process converges rapidly.

The previous scheme to select the PCF parameters to tailor a ultraflattened dispersion profile can be easily formulated in terms of an optimization algorithm. Current work is being developed to automatize both the design and the fine-tuning processes into a fully integrated software optimization tool.

3 Some Specific Designs

We start by studying of configurations designed to have ultraflattened dispersion in the region around $1.55\,\mu$m. Using the procedure described in the previous section, it is possible to systematically obtain ultraflattened dispersion configurations using $1.55\,\mu$m as the reference wavelength providing the magnification M. These configurations can be designed to show positive, negative or nearly-zero D just by properly adjusting the value of the filling fraction f. However, despite the dispersion profiles obtained this way are certainly ultraflattened, they are not necessarily optimized. This means that they will not provide the widest windows of ultraflattened behavior. Nevertheless, they constitute a good starting point to search configurations with optimal width at a given D.

Even without a sophisticated optimization algorithm, we can take advantage of the non-optimized profiles provided by the procedure described in the previous sections to obtain improved ultraflattened profiles. In Fig. 4 we show three curves characterized for having negative, nearly-zero, and positive dispersion coefficient D. We would like to point out that it is easier to achieve broader wavelength windows for ultraflattened curves with positive dispersion. This feature can be understood by analyzing the way they are obtained in the design process. If we look at the material dispersion in Fig. 3, we see that it is precisely in this region where $-D_{\mathrm{m}}$ behaves more smoothly, thus providing a larger wavelength interval of linear behavior. On the other hand, we need D_{g} curves with the same slope as the $-D_{\mathrm{m}}$ curve at the reference wavelength but, and this is the crucial point, that simultaneously remain above it. This means we need to use curves corresponding to higher filling fraction in Fig. 2(b) to achieve increasingly higher positive values of D. This is so because the larger f is, the more shifted to higher λ's these curves are, and, consequently, the higher the total dispersion becomes. However, this is not the only effect that occurs as f increases. It turns out that the linear part of these curves also increases when shifted to higher λ's, as depicted in Fig. 2(b). As a consequence, the overlapping region of linear behavior of the $-D_{\mathrm{m}}$ and D_{g} curves

#37487 - $15.00 US Received November 05, 2001; Revised December 05, 2001

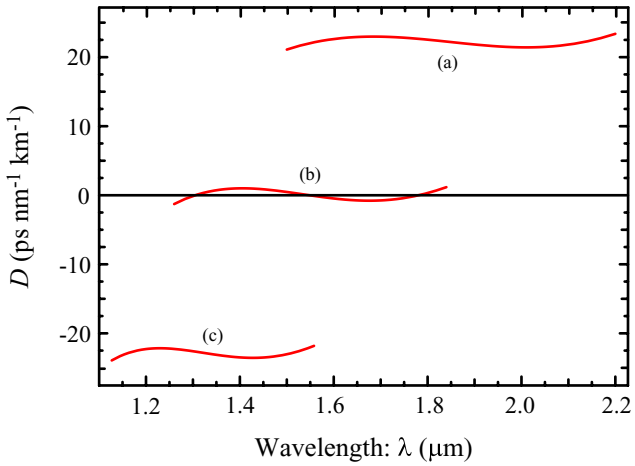

Fig. 4. Ultraflattened dispersion behavior for three different PCF configurations near the communication window with: (a) positive dispersion ($a = 0.4\,\mu$m and $\Lambda = 3.12\,\mu$m); (b) nearly-zero dispersion ($a = 0.316\,\mu$m and $\Lambda = 2.62\,\mu$m); and (c) negative dispersion ($a = 0.27\,\mu$m and $\Lambda = 2.19\,\mu$m). The ultraflattened behavior bandwidth, that corresponds to an allowed dispersion variation of $2\,\mathrm{ps\,nm^{-1}\,km^{-1}}$, is 668 nm, 523 nm, and 411 nm, respectively.

potentially becomes larger as D increases. The final outcome is a wider ultraflattened dispersion profiles for higher positive D's, as shown in Fig. 4. An analogous, but opposite, argument can be used to show why the wavelength windows of ultraflattened dispersion behavior get reduced as we search configurations with increasingly negative dispersion, as it is apparent in Fig. 4 as well. In any case, notice the remarkably wide windows of ultraflattened dispersion behavior. These windows are defined according to the usual criterion used to define flattened dispersion, namely, that the maximum of the dispersion variation in the given window has to be lesser than a fixed small amount (in our case, $2\,\mathrm{ps\,nm^{-1}\,km^{-1}}$).

The reduction of the ultraflattened dispersion window for shorter wavelengths has its main origin in the $-D_\mathrm{m}$ curve behavior that becomes less and less smooth as we decrease λ due to its growing curvature. The slope of this curve increases quickly yielding smaller wavelength regions where the overlap of the intervals of linear behavior of $-D_\mathrm{m}$ and D_g can occur. So, it is clear that there exist a limit for ultraflattened behavior as we move toward shorter wavelengths. If λ is small enough, the behavior of the material dispersion is so badly represented by a linear approximation that there is not even the possibility to work with the same design procedure explained in the previous section to obtain ultraflattened dispersion profiles. This is the case of the *Ti-Za* wavelength window centered at $0.8\,\mu$m.

The strategy to pursue in such a situation has to be necessarily different altough based on similar ideas. This strategy is based upon the two following observations. The first one is that the value of $-D_\mathrm{m}$ for silica at $0.8\,\mu$m is approximately $120\,\mathrm{ps\,nm^{-1}\,km^{-1}}$, a high value to compensate with D_g if one is looking for positive or nearly zero total dispersion. The second one is that, in this wavelength range, the curvature of the geometrical and material curves, unlike in the $1.55\,\mu$m region, has always opposite signs. This fact is clearly appreciated in Fig. 2, where the curvature of D_g is negative around $0.8\,\mu$m in all cases, whereas, according to Fig. 3, the curvature of $-D_\mathrm{m}$ remains positive even for values of λ beyond the zero material dispersion point at $1.3\,\mu$m. The issue now is not to play with the slope of D_g, as before, but to be able to achieve values of the geometrical dispersion large enough to compensate for the high value of the sign-changed

#37487 - $15.00 US
Received November 05, 2001; Revised December 05, 2001

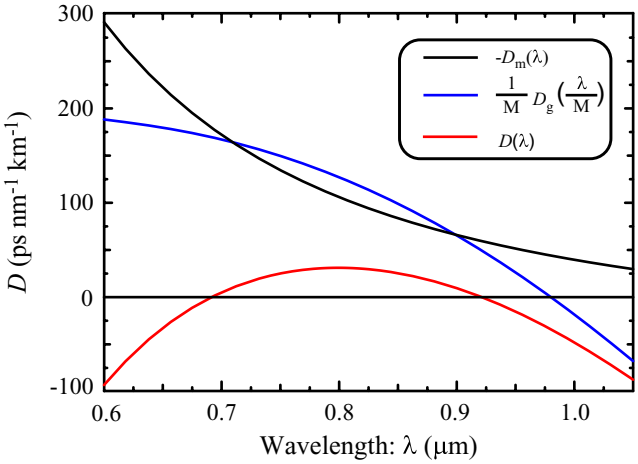

Fig. 5. As in Fig. 3 but for a typical case exhibiting positive flattened dispersion in the 0.8 μm window.

material dispersion at this wavelength. Our strategy will consist in finding configurations whose geometrical dispersion around 0.8 μm exceeds the value of $-D_{\rm m}$ in the same wavelength region, as shown in Fig. 5. Because of the opposite sign of the curvature of these two curves, it is granted that the profile of the total dispersion will have the form shown by the red curve in Fig. 5. It will include one point of zero third-order dispersion, located at the wavelength for which the difference between the $D_{\rm g}$ and $-D_{\rm m}$ curves reaches a maximum, or, equivalently, at the point for which the negative slopes of both curves are equal. This type of behavior has been already proven to exist in PCF's, although in a different wavelength window and only for nearly-zero dispersion [5].

We start with our reference configuration curve (that with $M = 1$, or $\Lambda = 2.3\,\mu$m, in Fig. 2 (a)), whose maximum occurs close to 0.8 μm. At this wavelength, the geometrical dispersion has a small value ($D_{\rm g} \approx 25\,{\rm ps\,nm^{-1}\,km^{-1}}$) as compared to that of $-D_{\rm m}$ at the same wavelength. The properties depicted in Fig. 2 for $D_{\rm g}$ will guide us in increasing the values of the geometrical dispersion. According to Fig. 5, we will focus on the region of these curves that have negative slope and near maximum. It is clear from Fig. 2(b) that, as we increase f, the maximum of the $D_{\rm g}$ curve moves upwards and simultaneously is shifted to the right. Despite that we are able to increase the value of the maximum of the $D_{\rm g}$ curve, this maximum moves away from the 0.8 μm window. We can relocate the $D_{\rm g}$ curve in such a way the region near maximum moves back to the desired window by acting now on the magnification M. By reducing M, we simultaneously displace the maximum to shorter wavelengths and increase its value, as depicted in Fig. 2(a). The global effect on the value of the dispersion of this twofold operation is additive, so that we can considerably increase the value of the geometrical dispersion in the 0.8 μm window by a suitable selection first of f (increase) and then of M (decrease). The high value of $-D_{\rm m}$ at 0.8 μm can be in fact overcome, as shown by the positive dispersion curve in Fig. 6.

We have already shown the existence of configurations that exhibit ultraflattened dispersion behavior in regions including 1.5 μm (Fig. 5). Another complementary question we can formulate now is whether it is possible to obtain also flattened dispersion configurations in windows centered at 1.5 μm. The answer to this question is certainly yes. It is not surprising because, according to what it has been discussed before for the 0.8 μm window, the requirement for flattened dispersion behavior is less demanding than that necessary to achieve an ultraflattened dispersion profile. Therefore, it is possible

#37487 - $15.00 US
Received November 05, 2001; Revised December 05, 2001

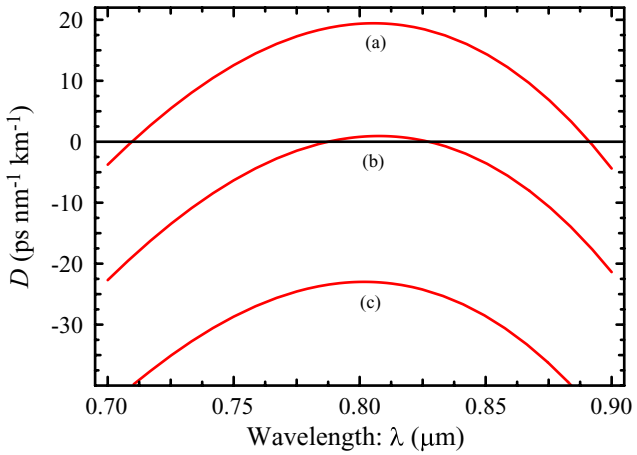

Fig. 6. Flattened dispersion behavior for three different PCF configurations centered near the *Ti-Za* window at 0.8 μm: (a) with positive dispersion ($a = 0.28\,\mu m$ and $\Lambda = 0.88\,\mu m$); (b) with nearly-zero dispersion ($a = 0.27\,\mu m$ and $\Lambda = 0.90\,\mu m$); and (c) with negative dispersion ($a = 0.255\,\mu m$ and $\Lambda = 0.91\,\mu m$). The allowed variation of the flattened dispersion profiles is $2\,\mathrm{ps\,nm^{-1}\,km^{-1}}$ and their corresponding flattened dispersion bandwidths are 58 nm, 57 nm, and 59 nm, respectively.

to analyze the interesting technological issue of the tunableness of flattened dispersion in the telecommunication window centered at 1.5 μm. In another words, we search all type of flattened dispersion configurations that can have positive, negative, or nearly-zero dispersion centered at this wavelength. In this way, we will be able to identify the PCF's geometrical parameters that permit to tailor an specified flattened dispersion profile in this window. This is precisely the analysis depicted in Fig. 7. We can appreciate here that there is a considerable range of tunableness in the dispersion of a PCF in this window. This range extends from configurations owning positive dispersion (up to $+45\,\mathrm{ps\,nm^{-1}\,km^{-1}}$) to configurations with similar but negative value of dispersion (up to $-43\,\mathrm{ps\,nm^{-1}\,km^{-1}}$). In all cases, the wavelength extension of the flattened dispersion behavior is around or above 200 nm.

4 Conclusions

We have demonstrated how a smart utilization of the geometry of the photonic crystal cladding of a triangular PCF permits an outstanding control of the dispersion properties of the fiber. The fact that the geometrically-induced dispersion of a PCF has remarkable properties and it is highly tunable in terms of the geometrical parameters of the fiber can be used to properly compensate the inherent dispersion of the silica in many different ways. The key point is the understanding of the interplay between both type of dispersions, which is easily achieved by means of a suitable graphical representation and the use of the approximate equation for the total dispersion given in Ref. (2). As a result, we have been able to establish a well-defined prescription to design a wide variety of dispersion behaviors in the telecommunication and the *Ti-Za* windows. We have focused on a specially technologically interesting type of dispersion profiles, namely, that corresponding to configurations owning constant dispersion over wide wavelength windows. In this direction, we have formulated two different design procedures depending on whether we are interested to achieve flattened dispersion (one point of zero third-order dispersion) or ultraflattened dispersion (one point of zero fourth-order dispersion). In all cases, the basic triangular geometry of the PCF cladding has proven to be very rich in yielding configurations covering a large dispersion spectrum, ranging from rather

#37487 - $15.00 US
Received November 05, 2001; Revised December 05, 2001

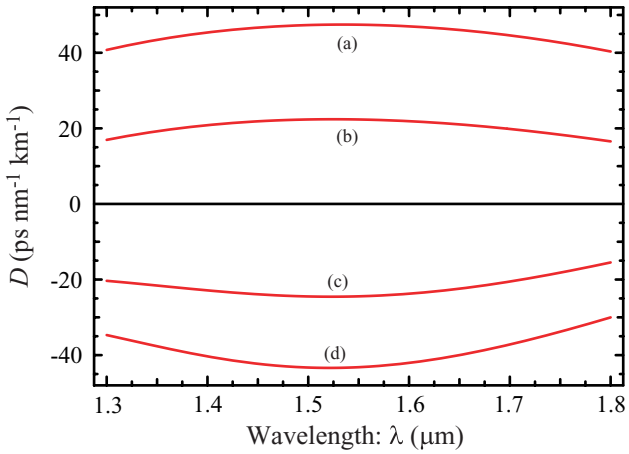

Fig. 7. Four flattened dispersion curves corresponding to different values of the dispersion centered near $1.55\,\mu$m. With positive dispersion: (a) $D \approx +45\,\mathrm{ps\,nm^{-1}\,km^{-1}}$ with $a = 0.49\,\mu$m and $\Lambda = 2.32\,\mu$m, and (b) $D \approx +22\,\mathrm{ps\,nm^{-1}\,km^{-1}}$ with $a = 0.40\,\mu$m and $\Lambda = 2.71\,\mu$m. With negative dispersion: (c) $D \approx -23\,\mathrm{ps\,nm^{-1}\,km^{-1}}$ with $a = 0.28\,\mu$m and $\Lambda = 2.16\,\mu$m, and (d) $D \approx -43\,\mathrm{ps\,nm^{-1}\,km^{-1}}$ with $a = 0.27\,\mu$m and $\Lambda = 1.93\,\mu$m. The allowed variation of the flattened dispersion profiles is $2\,\mathrm{ps\,nm^{-1}\,km^{-1}}$ and their corresponding flattened dispersion bandwidths are 270 nm, 294 nm, 259 nm, and 195 nm, respectively.

large positive values to equally large negative values of dispersion. The final conclusion of our systematic analysis on PCF dispersion is that, despite the enormous size of the parameter space, a good comprehension of the guidance mechanism permits an extreme simplification of the search procedure, resulting in the implementation of a successful design prescription to achieve constant dispersion configurations.

This research was supported by the Plan Nacional I+D+I (grant TIC2001-2895-C02-02), Ministerio de Ciencia y Tecnología, Spain.

#37487 - $15.00 US
Received November 05, 2001; Revised December 05, 2001